

Kinetics of Surface-Bound Benzo[*a*]pyrene and Ozone on Solid Organic and Salt Aerosols

Nana-Owusua A. Kwamena,[†] Joel A. Thornton,^{†,‡} and Jonathan P. D. Abbatt^{*,†}

Department of Chemistry, University of Toronto, Toronto, Ontario M5S 3H6, Canada

Received: August 25, 2004; In Final Form: October 15, 2004

An aerosol flow tube apparatus was developed to perform the first kinetic study of the oxidation of particulate-bound BaP on solid organic and salt aerosols by gas-phase ozone. The studies on azelaic acid aerosols were performed with submonolayer coatings of BaP under both dry (RH < 1%) and high relative humidity (RH ~ 72%) conditions. The reaction exhibited pseudo-first-order kinetics for BaP loss and the pseudo-first-order rate coefficients displayed a Langmuir–Hinshelwood dependence on gas-phase ozone concentration. Under high relative humidity conditions the kinetics were faster but also displayed a similar functional dependence on the gas-phase ozone concentration. By assuming Langmuir–Hinshelwood behavior, the following parameters were obtained: ozone-surface equilibrium constant $K_{O_3}(< 1\% \text{ RH}) = (1.2 \pm 0.4) \times 10^{-15} \text{ cm}^{-3}$, $K_{O_3}(72\% \text{ RH}) = (2.8 \pm 1.4) \times 10^{-15} \text{ cm}^{-3}$, the maximum pseudo-first-order rate coefficient $k_{\text{max}}^1(< 1\% \text{ RH}) = (0.048 \pm 0.008) \text{ s}^{-1}$, $k_{\text{max}}^1(72\% \text{ RH}) = (0.060 \pm 0.018) \text{ s}^{-1}$. Uptake coefficients were extracted from the pseudo-first-order rate coefficients and a slight trend of decreasing uptake coefficients with increasing ozone concentration was observed. In contrast to the behavior on azelaic acid aerosols, no reaction was observed between ozone and BaP adsorbed to solid NaCl particles. These results are compared to previous studies, which have been performed on different substrates, and their atmospheric implications are discussed. We conclude that a strong substrate effect prevails in this reaction with the kinetics proceeding faster on surfaces best able to adsorb ozone.

1. Introduction

Polycyclic aromatic hydrocarbons (PAHs) are emitted into the atmosphere from combustion sources and many are known carcinogens. Larger PAHs, such as benzo[*a*]pyrene (BaP), partition to fine particulate matter because of their low vapor pressures. This particulate matter can penetrate deep into the lungs resulting in allergenic, mutagenic and carcinogenic responses.¹ Recent studies have shown a link between increases in PM_{2.5} and increases in hospital admissions.² Furthermore, the oxidation products may be even more mutagenic or carcinogenic than the parent PAHs.^{3,4} Therefore, it is necessary to characterize the chemical and physical mechanisms that control the fate and transport of atmospheric PAHs to determine any aerosol-related health risks and improve urban air quality.

The fate of gas-phase PAHs is primarily determined by their reactions with atmospheric oxidants such as OH, O₃, NO_x, and SO_x. However, heterogeneous reactions between surface-bound PAHs and gas-phase oxidants govern the fate of the higher molecular weight PAHs. The interaction between the particle and the chemical species adsorbed to it may alter the mechanism and reaction cross section relative to its behavior in the gas phase, and it may also change the microphysical properties of the particle itself. For example, the reactions of surface-bound organics may change the surficial properties of the particle by making it more hygroscopic, therefore enhancing its cloud nucleation properties.⁵

The gas-phase reactions of organics such as PAHs have been the focus of past atmospheric research. However, changes to

particle-bound organics have not been studied to the same extent.⁶ Furthermore, there is much variability regarding the reactivity of surface-bound BaP in the literature, which may be attributed to the different substrates, analytical methods and PAH and atmospheric oxidant concentrations that have been used in the various studies. As examples, Lane and Katz⁷ studied the surface reactions of BaP on Petri dishes and found BaP to be highly reactive to ozone in the dark after 3.5 h of exposure. However, work done by Grosjean and co-workers⁸ on a variety of substrates (from glass fiber filters to ambient air particles) observed no BaP degradation after 3 h exposures to ozone. Work by Korfmacher et al.⁹ demonstrated a possible substrate effect on the photochemical decomposition of PAHs adsorbed to coal fly ash and alumina. They found BaP adsorbed to coal fly ash to be highly resistant to photodecomposition. However, when experiments were performed on alumina TLC plates, a 40–50% loss of the initial BaP amount was observed after 80 min of light exposure. It is unclear whether these effects depend on the physical or chemical nature of the underlying surface.

Other studies have shown that the amount of BaP surface coverage could also influence the rates of reaction.^{9–12} Alebic-Juretic et al.¹⁰ found that the first-order rate constants for BaP on silica gel exposed to ozone were more than twice as fast for less than monolayer coverage compared to greater than monolayer coverage. Likewise, Kamens et al.¹³ observed similar results for PAH decay on atmospheric soot particles exposed to ozone. One explanation that has been proposed is that the oxidation products, which have lower volatility than the parent PAH, prevent the oxidant from reaching the BaP that is buried underneath when there is greater than monolayer coverage of PAHs.¹¹

Past kinetic studies have also provided clues about the reaction mechanism between surface-bound BaP and gas-phase

* To whom correspondence should be addressed. E-mail: jabbatt@chem.utoronto.ca.

[†] University of Toronto.

[‡] Currently at the Department of Atmospheric Sciences, University of Washington, Seattle, WA 98195-1640.

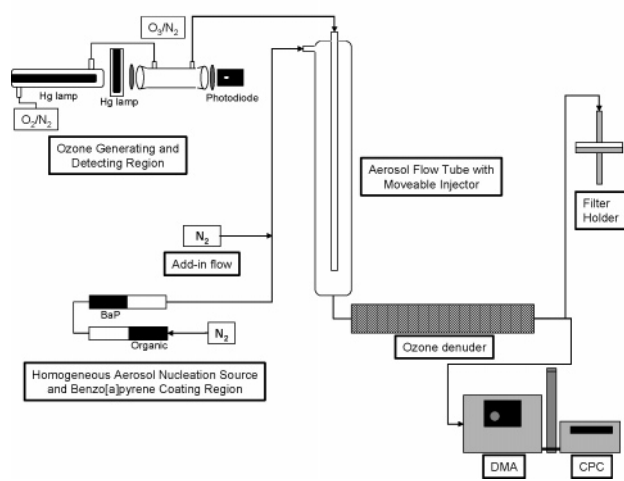


Figure 1. Experimental setup for the kinetic experiments of surface-bound BaP on organic aerosols. Following filter collection, the filters were extracted ultrasonically and analyzed using HPLC with fluorescence detection to monitor the BaP concentration. Dry inorganic aerosols were generated by atomizing a dilute solution of sodium chloride and passing the aerosols through a diffusion dryer.

ozone. Studies by Alebic-Juretic et al.¹⁰ and Wu et al.¹¹ revealed a linear dependence between the observed first-order rate coefficient and ozone concentration. This linear dependence suggests a simple bimolecular reaction between the surface-adsorbed BaP and ozone. However, recent studies by Poschl et al.¹⁴ and Mmerekki et al.¹⁵ suggest that reactions of this nature proceed via a Langmuir–Hinshelwood reaction mechanism where ozone adsorbs to the surface prior to reacting with the BaP.

Aside from the concentration and nature of the oxidant, the atmospheric lifetimes of surface-adsorbed species may depend on a variety of factors including the relative humidity and the nature of the particle substrate. Taken together with the dependence on surface coverage, it is clear that accurate atmospheric modeling of the kinetic behavior of surface-bound PAHs requires further laboratory studies. In light of these issues, we have undertaken a kinetic study of the oxidation of BaP bound to the surface of solid organic and salt aerosols. Experiments were performed to examine the kinetics between surface-bound BaP and gas-phase ozone as a function of aerosol substrate, gas-phase ozone concentration, and relative humidity. We believe this to be the first such study on these substrates in the submonolayer surface coverage regime. In part, this work and experimental approach were motivated by the analogous study of BaP oxidation on graphitic particles recently performed by Poschl et al.¹⁴

2. Experimental Section

2.1. Aerosol Generation and Coating. An analytical technique was developed to investigate the reaction between ozone and surface-bound benzo[a]pyrene (BaP) at submonolayer coverage on solid organic and salt aerosols under dry and high relative humidity conditions. Figure 1 provides a schematic of the experimental setup used for examining the kinetics of surface-bound BaP on solid organic aerosols under dry conditions. Azelaic acid aerosols, which were used as the model for the solid organic aerosols, were generated by homogeneous nucleation. A mass flow controller (MKS Inc.) was used to send a volumetric flow of 0.3 lpm of N₂ through a 30.5 cm Pyrex tube containing azelaic acid (98%, Sigma Aldrich). The Pyrex

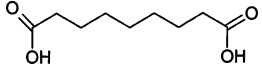
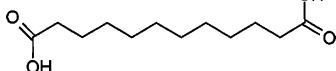
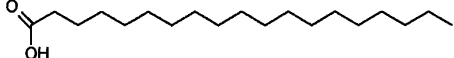
tube was wrapped in heating tape and connected to a Variac. The particles nucleated as the heated flow entered the room-temperature Teflon tubes. Particles were coated with BaP by sending the resulting aerosol flow through a second 30.5 cm heated Pyrex tube containing BaP, similar to the first. The flow of azelaic acid aerosols became enhanced with BaP vapor when the second tube was heated. Similarly, as this flow encountered the cooler Teflon tubes, BaP condensed onto the existing azelaic acid aerosols. The aerosol BaP fractional surface coverage was controlled by adjusting the temperature of the BaP coating region. All kinetic experiments were run with the following conditions: BaP coating region temperature $T_{\text{BaP}} = 339$ or 349 K. The flow tube temperature was (298 ± 5) K. The particle number density in the flow tube was approximately 10^5 cm^{-3} . The median diameter of the aerosols was approximately 98 nm with a geometric standard deviation of $\sigma_d = 1.36$.

To study the reaction of surface-bound BaP in the presence of ozone, an aerosol substrate that was not prone to ozonation was chosen. Saturated carboxylic acids are known to have little to no reactivity with ozone and they are ubiquitous throughout the troposphere. We view the acids as the surrogate for the oxygenated organic component of solid tropospheric aerosols but not of any low volatility hydrocarbon fraction. Three carboxylic acids—azelaic acid, stearic acid, and dodecanedioic acid—were explored as possible aerosol substrates. Table 1 describes their chemical and physical characteristics. There is no vapor pressure listed for dodecanedioic acid, but based on its chemical structure, it can be assumed that its vapor pressure should be lower than that of azelaic acid.

Experiments were performed to evaluate the suitability of each of the acids as potential organic aerosol substrates. A differential mobility analyzer (DMA) and condensation particle counter (CPC) were used to compare the size, distribution, and surface area of each carboxylic acid aerosol population as it passed through an unheated and heated second region. An aerosol substrate that yielded submicron sized particles with high surface area for the BaP to partition onto was desired. Furthermore, it was necessary for the particles to have low volatility as they passed through the heated BaP coating region to minimize particle evaporation.

As shown in Figure 2, the stearic acid aerosol size distribution changed as the particles passed through a second heated region at 338 K compared to when that region was at room temperature. The mean diameter of this aerosol population was smaller in size suggesting that the particles may have evaporated and recondensed to form new smaller-sized particles. In contrast, when azelaic acid aerosols passed through a second heated region, there was only a minor change in the aerosol size distribution with a small loss of the larger sized particles. We note, however, that there may be changes in the aerosol distribution due to convection driven depositional processes, and so we view this small size change as insignificant. Dodecanedioic acid aerosols (not shown) showed similar behavior to the azelaic acid aerosols. Therefore, prior to performing kinetic studies between surface-bound BaP and ozone, we performed experiments to compare the stability of the BaP surface concentration of both azelaic acid and dodecanedioic acid aerosols as a function of time. Even though dodecanedioic acid has the lowest volatility, azelaic acid was chosen as the organic acid aerosol substrate because the dodecanedioic acid particle number concentration was variable with time. The exact reason for this behavior is not clear. However, azelaic acid's aerosol distribution was largely invariant with time, therefore, demonstrating the stability of the azelaic acid aerosol source.

TABLE 1: Chemical and Physical Properties of the Three Organic Acids Investigated as Aerosol Substrates

name	molecular weight (g/mol)	vapor pressure at 298 K ¹⁶ (Pa)	structure
azelaic acid (nonanedioic acid)	188.21	8.80×10^{-6}	
dodecanedioic acid	230.31	N/A	
stearic acid (octadecanoic acid)	284.48	2.76×10^{-4}	

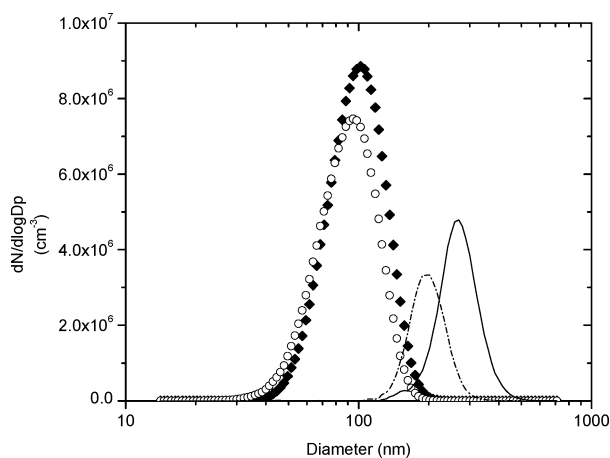


Figure 2. Comparison of azelaic acid and stearic acid aerosol distributions after passing through a second heated region. Azelaic acid aerosols through the BaP coating region at room temperature (black diamonds) and at 338K (open circles). Stearic acid aerosols through BaP region at room temperature (solid line) and at 338 K (dash dotted line).

Given that we heat to deposit BaP as a surface layer, we acknowledge that azelaic acid particles may volatilize to some degree in the BaP coating region. Specifically, for our highest operating temperature (349 K), the vapor pressure of azelaic acid was determined to be 0.0187 Pa.¹⁶ For a typical average aerosol surface area concentration of 4×10^{10} nm²/cm³, 0.3 lpm through the aerosol generating tube, and a total of 1.9 lpm through the main aerosol flow tube, the maximum number of azelaic acid molecules that may evaporate and recondense is approximately 2×10^{15} cm⁻². This is close to but slightly larger than a monolayer. However, this assumes that the flow becomes saturated with azelaic acid vapor, that all this vapor condenses onto the particles upon cooling and not onto the Pyrex tube walls and that the particles are smooth at the molecular level. In our kinetic studies we performed experiments at two different operating temperatures for BaP coating to investigate if burial of BaP by recondensing azelaic acid was an issue.

2.2. Aerosol Flow Reactor. Dry N₂ (1.5 lpm) was added using a mass flow meter (MKS Inc.) to make the total flow through the vertically oriented Pyrex aerosol flow tube (id 6 cm, length 96 cm) 1.9 lpm. The aerosol flow tube was operated under laminar flow conditions at ambient pressure and temperature (1 atm, 298 K, Reynolds number \sim 46). For the high relative humidity (RH = 72%) experiments, a fraction of the add-in flow (\sim 1.2 lpm) was sent through a water bubbler. The remaining portion was made up by adding dry N₂ (\sim 0.3 lpm). A hygrometer (VWR International), placed before the flow tube, was used to determine the relative humidity of the total flow entering the flow tube. The kinetic experiments performed at

high relative humidities were carried out in the dark to eliminate possible reactions with OH arising from O₃ and H₂O photochemistry.

Ozone was generated by ultraviolet irradiation of a mixed flow (total flow: \sim 0.09 lpm) of O₂ and N₂ by a mercury pen-ray lamp (length: 9", UVP Inc) in a homemade Pyrex glass chamber. The ozone concentration was controlled by varying the ratio of O₂ to N₂ passing over the pen-ray lamp. Ozone was detected using a second mercury pen-ray lamp (length: 2.12", UVP Inc) placed in front of a homemade 10.3 or 50 cm absorbance cell with quartz windows at either end. An interference filter (Escoproducts) was placed in front of an ultraviolet sensitive photodiode (Boston Electronics Corp.) at the other end of the absorbance cell to determine the ozone concentration entering the aerosol flow tube. Ozone was introduced into the flow tube through a moveable Pyrex rod injector, which split into four prongs at the end to facilitate rapid mixing of the ozone into the total flow. The flow tube ozone concentrations investigated under dry and 72% RH conditions were 0–1.11 $\times 10^{15}$ molecules/cm³ and 0–8.86 $\times 10^{14}$ molecules/cm³, respectively. The reaction time (up to 70 s) between ozone and surface-bound BaP was varied by setting the injector to different positions (0–76 cm) along the length of the flow tube. We assume that the reaction times were determined by the total bulk velocity since full mixing of the ozone into the bulk flow should occur on the time scale of roughly 10 s via molecular diffusion.

The number of kinetic points obtained for a given kinetic decay was dependent on the ozone concentration being investigated. At higher ozone concentrations, the surface-bound BaP was consumed faster, quickly approaching our analytical detection limit for longer reaction times. As a result, the number of points for a kinetic run was reduced compared to those experiments performed at lower ozone concentrations. Nonetheless, all kinetic measurements were performed following the same procedure. Prior to turning on the ozone generating lamp, a sample was collected with the injector at the 0 cm sampling position. The kinetic study was begun by turning on the ozone generating lamp. Duplicate filter samples were taken at six different injector sampling positions between 0 and 76 cm. Aerosols were collected for 6.5 min on glass fiber filters (GF/A 47 mm, Whatman), which were mounted on a homemade stainless steel filter holder positioned after the ozone denuder. At the end of the experiment, the ozone generating lamp was turned off and another sample was taken at the 0 cm sampling position. The error for each point was determined by taking the variability in the replicate measurements at each injector position. For the experiments performed at high relative humidities, filter collection was done in the same manner.

The reaction between BaP and ozone was stopped using an ozone denuder positioned immediately after the flow tube. The denuder was homemade consisting of an outer Pyrex tube

(length 100 cm), with an inner stainless steel mesh tube (od 1/2", length 100 cm). Carulite (Carus), a mixture of manganese dioxide and copper dioxide, was placed in the sleeve between the Pyrex and the mesh to catalytically remove the ozone. The denuder was able to remove at least 99% of the ozone in the flow. Following the denuder, part of the aerosol flow (1.5 lpm) was diverted to a glass fiber filter for aerosol collection. This flow was then vented into the laboratory's main exhaust line. The remaining aerosol flow was sent to a differential mobility analyzer (TSI Inc, model 3080) connected to a condensation particle counter (TSI Inc, model 3010), which were used to monitor the aerosol size distributions. The DMA/CPC measurements were simultaneously obtained with the aerosol filter collection.

Minor changes to the system's set up were made for the analysis of the degradation of BaP on solid sodium chloride aerosols, which were used as the model salt aerosols. These aerosols were generated by atomizing (TSI Inc, model 3076) a dilute solution of sodium chloride (1 wt %) and effloresced by passing the flow (0.5–0.7 lpm) through a diffusion dryer (TSI Inc, model 3062). The salt aerosol was coated with BaP as previously described. Dry N₂ was added to make the total flow ~1.9 lpm. A mass flow meter (MKS Inc., Massachusetts), needle valve (Hoke Inc.), and diaphragm pump (Thomas Industries Inc.) were placed on the other side of the filter holder to draw a constant fraction of the flow tube output. The remaining flow (0.3 lpm) was sent to the DMA/CPC to monitor the aerosol size distribution.

2.3. Aerosol Sampling and Analytical Methods. The kinetics between surface-bound BaP and O₃ were determined by monitoring the amount of unreacted BaP on the aerosols. Following collection, the filters were placed in amber screw top vials and refrigerated at 277 K until analysis. The filters were ultrasonically extracted twice with dichloromethane (99.9% HPLC grade, Sigma-Aldrich). The extracts were transferred to conical vials (15 mL Falcon tubes, Becton Dickinson Labware) and evaporated to dryness under a gentle stream of nitrogen gas. The samples were reconstituted in 0.5 mL of acetonitrile (HPLC grade, Fischer Scientific) and analyzed by high performance liquid chromatography (HPLC) with fluorescence detection. An HPLC system from Perkin-Elmer (Series 200 LC pump) was interfaced to a fluorescence detector (LC-240, Perkin-Elmer) and an autosampler (Advanced LC Sample Processor ISS 200, Perkin-Elmer). The system was equipped with a C-18 guard column (Adsorbosil, 5 μm, 7.5 × 4.6 mm, Alltech) coupled to a C-18 reversed-phase chromatographic column (Spheri-5, 220 × 4.6 mm, Brownlee Labs). Analysis was performed using a 10 μL injection volume and an isocratic elution of acetonitrile–water (97:3 v/v, HPLC grade Fischer Scientific and 18 MΩ water, respectively) at a constant flow rate of 1 mL min⁻¹. The excitation/detection wavelength pair of 297/404 nm was used to monitor the BaP signal. The Turbochrom software package (Perkin-Elmer) was used to integrate the chromatographic peaks. The degradation of BaP was quantified using an external standards calibration of BaP standard solutions ranging from a few ppb to a few ppm, which was run along with each kinetic analysis. The BaP detection limit was 1.2 ppb. Spike and recovery experiments on BaP revealed a BaP recovery of 60%. Therefore, HPLC peak areas were corrected for 100% recovery before quantification with the calibration curve.

3. Results

3.1. Benzo[a]pyrene Surface Concentration on Organic and Inorganic Aerosols.

The BaP surface concentration on

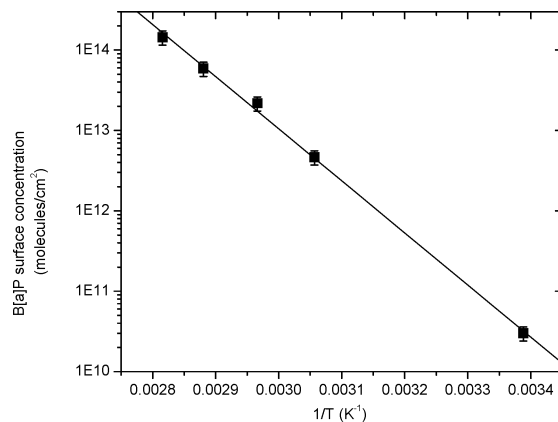


Figure 3. Variation of the BaP surface coverage with temperature of the BaP coating region. Applying the Clausius–Clapeyron equation, an experimental sublimation enthalpy of (124 ± 3) kJ mol⁻¹ was obtained. This is in good agreement with the literature¹⁸ value (118 ± 2) kJ mol⁻¹ and the work done by Poschl et al.¹⁴ on soot aerosols (118 ± 5) kJ mol⁻¹.

organic and inorganic aerosols is defined as the number of BaP molecules per square centimeter of aerosol surface (cm⁻²) for a given filter sample. The aerosol surface area concentration (nm²/cm³) was obtained from the DMA/CPC measurements, which were taken simultaneously as the aerosols were being collected on the filter paper. The total aerosol surface area for a given filter sample was determined by knowing the flow (lpm) to the filter holder and the time for aerosol collection. The BaP signal obtained from the HPLC analysis was converted to the number of BaP molecules by interpolation of a BaP external standards calibration curve. Therefore, the BaP surface concentration ($[\text{BaP}]_{\text{surf}}$) was obtained by dividing the number of BaP molecules (N_{BaP}) by the total aerosol surface area (SA_{tot})

$$[\text{BaP}]_{\text{surf}} = \frac{N_{\text{BaP}}}{SA_{\text{tot}}} \quad (1)$$

The BaP surface coverage in monolayer units (θ_{BaP}) was determined by dividing the initial BaP surface concentration $[\text{BaP}]_{\text{surf}}$, in the absence of ozone, by the amount required for a full BaP monolayer

$$\theta_{\text{BaP}} = \frac{[\text{BaP}]_{\text{surf}}}{\sigma_{\text{BaP}}} \quad (2)$$

where σ_{BaP} is a monolayer of BaP, which was assumed to be 1×10^{14} cm⁻² based on its molecular cross section.¹⁷ We assumed that the particles were smooth at the molecular level. If they are not, then our monolayer coverages are upper limits to the true coverages.

3.2. Fractional Surface Coverage of Benzo[a]pyrene on Organic Aerosols. Previous studies have shown that the amount of BaP surface coverage (i.e., number of monolayers) may influence reaction rates.^{10,11} Therefore, azelaic acid aerosols were sent through the BaP coating region with temperatures ranging from 298 to 355 K allowing us to control the BaP surface coverage on the aerosols from sub to greater than monolayer coverage. The slope of the least squares plot of the BaP surface concentration as a function of inverse temperature of the BaP coating region (Figure 3) provided the sublimation enthalpy based on the Clausius–Clapeyron equation. In applying this equation, it was assumed that the carrier gas in the BaP coating region was saturated with BaP vapor. An experimental value of (124 ± 3) kJ/mol was obtained, which is in good agreement

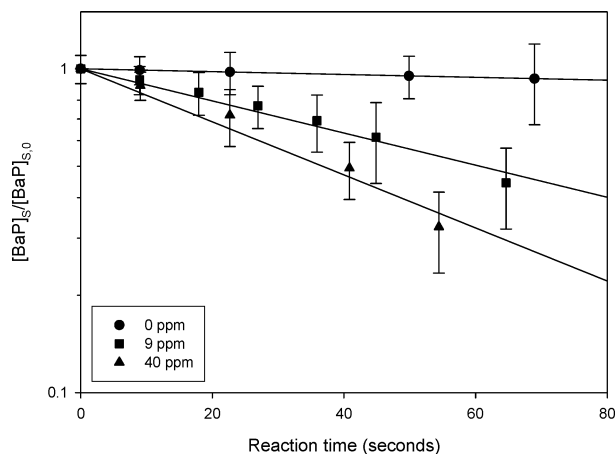


Figure 4. Kinetics at 0.5 monolayers of BaP on azelaic acid aerosols under dry conditions. Symbols indicate ozone mixing ratios.

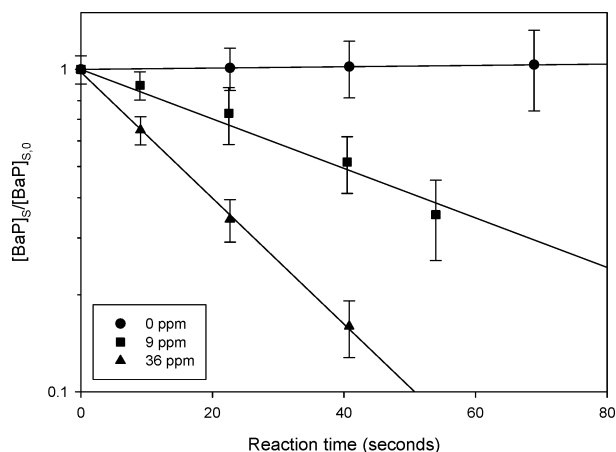


Figure 5. Kinetics at 0.04 monolayers of BaP on azelaic acid aerosols at 72% relative humidity. Symbols indicate ozone mixing ratios.

with that of Poschl et al.¹⁴ on soot aerosols (118 ± 5) kJ/mol and the extrapolated literature¹⁸ value (118 ± 2) kJ/mol.

3.3. Kinetics of Surface-Bound BaP on Solid Organic Aerosols under Dry and Wet Conditions. The reaction of surface-bound BaP on organic aerosols was investigated as a function of BaP fractional surface coverage, ozone concentration and relative humidity. The effect of the BaP fractional surface coverage was investigated by setting the temperature of the BaP coating region to either 339 or 349 K resulting in BaP surface coverages of 0.04 or 0.5 monolayers of BaP, respectively. The maximum number of azelaic acid molecules that may evaporate and recondense should be considerably lower at 339 K compared to 349 K, therefore, reducing the possibility of burial. The observed kinetics at the two BaP surface coverages were the same within the experimental precision of the current method. Therefore, we believe that burial of BaP by recondensing azelaic acid is of minimal significance for our studies.

Figures 4 and 5 show plots of the normalized BaP surface concentration as a function of reaction time under dry and 72% RH conditions. The reaction between surface-adsorbed BaP and ozone is well described by first-order kinetics given the linearity of the plots. The slope of the uncertainty-weighted, linear least-squares fit provided the pseudo-first-order rate coefficient (k_{obs}^1) at each ozone concentration studied. The uncertainty in this quantity was taken as the standard error in the slope of the plots at the 95% confidence interval. Note that there is minimal change to the BaP signal as a function of injector position with

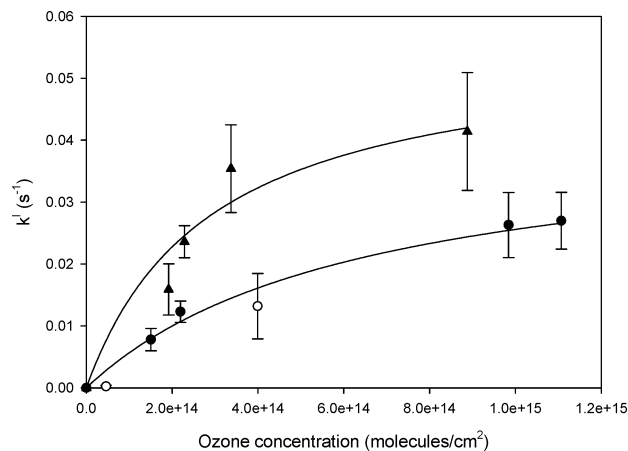


Figure 6. Pseudo-first-order rate coefficient as a function of gas-phase ozone concentration. Black circles: dry conditions with 0.5 monolayers of BaP; open circles: dry conditions with 0.04 monolayers of BaP; black triangles: at 72% relative humidity with 0.5 monolayers of BaP. The plots were fit using eq 4.

no ozone flowing, an indication that few aerosols are being lost along the length of the flow tube.

The plot of k_{obs}^1 as a function of flow-tube ozone concentration (Figure 6) is nonlinear with a shape that is consistent with the Langmuir–Hinshelwood reaction mechanism. The principles of the Langmuir–Hinshelwood model are similar to the Langmuir adsorption isotherm but apply to heterogeneous reactions. The Langmuir isotherm has three basic tenets including one that states that the adsorption of the gas-phase species cannot proceed beyond monolayer coverage.¹⁹ Therefore, in the Langmuir–Hinshelwood model, there are a limited number of sites available for the ozone to adsorb to and that saturation of the surface occurs at some gas-phase ozone concentration. At this point, the rate of the reaction should become independent of the ozone concentration, which is clearly demonstrated in Figure 6 as it appears as though the maximum pseudo-first-order rate coefficient plateaus at high ozone concentrations under both dry and high RH conditions. This is in contrast to an Eley–Rideal gas-surface reaction mechanism in which the first-order rate constant for BaP loss would scale linearly with the gas-phase ozone concentration.

The relationship between the k_{obs}^1 and the gas-phase ozone concentration can be modeled using the following which is based on the Langmuir equation:

$$k_{\text{obs}}^1 = \frac{k^{\text{II}}[\text{SS}]K_{\text{O}_3}[\text{O}_3]_{\text{g}}}{1 + K_{\text{O}_3}[\text{O}_3]_{\text{g}}} \quad (3)$$

where k^{II} is the second-order surficial rate coefficient, [SS] is the number of surface sites, K_{O_3} is the ozone gas-to-surface equilibrium constant, and $[\text{O}_3]_{\text{g}}$ is the gas-phase ozone concentration. From this equation, it is evident that k_{obs}^1 is dependent on both the number of surface sites and the gas-phase species concentration. This equation can be modified to yield the following:

$$k_{\text{obs}}^1 = \frac{k_{\text{max}}^1 K_{\text{O}_3} [\text{O}_3]_{\text{g}}}{1 + K_{\text{O}_3} [\text{O}_3]_{\text{g}}} \quad (4)$$

where k_{max}^1 is the maximum rate coefficient that would be observed at high ozone concentrations and it is a product of the second-order rate coefficient (k^{II}) and the number of surface

TABLE 2: Comparison of Adsorption Equilibrium Constants and the Maximum Pseudo-first Order Rate Coefficient

	substrate	PAH	K_{O_3} (10^{-13}cm^3)	k_{max}^I (s^{-1})
this work	azelaic acid aerosols (dry)	BaP	(0.012 ± 0.0004)	(0.048 ± 0.008)
	azelaic acid aerosols (wet)	BaP	(0.028 ± 0.014)	(0.060 ± 0.018)
this work	sodium chloride aerosols	BaP	$< 0.0012^b$	0.032^a
Poschl et al. ^c	soot aerosols	BaP	(2.8 ± 0.2)	(0.015 ± 0.001)
Wu et al. ^d	fused silica plates	BaP	0.28	0.032^a
Alebic-Juretic et al. ^e	nonactivated silica gel	BaP	0.095	0.032^a

^a The value for k_{max}^I was assumed to be 0.032s^{-1} , which is the average k_{max}^I of the results from this study and Poschl et al.¹⁴ ^b This was calculated assuming $k_1 = 3.0 \times 10^{-3}\text{s}^{-1}$, which value is the typical error of k^I obtained for azelaic acid aerosol kinetics under dry conditions. This value was taken to be the fastest kinetics that would have been observed on sodium chloride aerosols at the highest ozone concentration investigated (31 ppm). ^c Reference 14. ^d Reference 11. ^e Reference 10.

sites for the adsorbed species (i.e., BaP). The data in Figure 6 were fit using a nonlinear least-squares fit of eq 4 based on the Levenberg–Marquardt algorithm in the Origin 6.0 data analysis software package. The fitting parameters provided K_{O_3} and k_{max}^I as listed in Table 2. The error for these parameters was obtained from the statistical error of the nonlinear least-squares fit. The K_{O_3} was $(1.2 \pm 0.4) \times 10^{-15}\text{cm}^3$ and $(2.8 \pm 1.4) \times 10^{-15}\text{cm}^3$ at $<1\%$ RH and 72% RH, respectively. The k_{max}^I at $<1\%$ RH and 72% RH was $(0.048 \pm 0.008)\text{s}^{-1}$ and $(0.060 \pm 0.018)\text{s}^{-1}$, respectively.

The uptake coefficient (γ) is the ratio of the number of collisions that result in a reaction to the total number of collisions between a gas-phase molecule and a surface. For a simple bimolecular reaction mechanism the uptake coefficient is calculated as follows:

$$\gamma = \frac{4k^I}{\sigma_{\text{BaP}}\omega_{O_3}[\text{O}_3]} \quad (5)$$

where σ_{BaP} is the BaP molecular cross section and ω_{O_3} is the mean velocity of ozone. However, as derived by Poschl et al.¹⁴ and Amman et al.,²⁰ this equation must be modified when the reaction is described by the Langmuir–Hinshelwood model:

$$\gamma = \frac{4k_{\text{max}}^I K_{O_3}}{\sigma_{\text{BaP}}\omega_{O_3}(1 + K_{O_3}[\text{O}_3])} \quad (6)$$

The pseudo-first-order rate constants obtained in this work from the kinetic studies under both dry and high RH conditions were transformed into uptake coefficients using eq 5. The error of the uptake coefficients was taken as the standard error of k_{obs}^I at the 95% confidence interval. These uptake coefficients were plotted as a function of ozone concentration, as shown in Figure 7. The curve illustrating a trend of decreasing uptake coefficient with increasing ozone concentration was obtained from a nonlinear least-squares fit of eq 6. A comparison of the raw data and the best fit curve reveals only a small decrease in the uptake coefficient with increasing gas-phase ozone concentration. Under dry conditions, this decreasing trend starts with ozone concentrations greater than 2.19×10^{14} molecules/ cm^3 . For the kinetics performed at 72% RH, the trend starts at 3.9×10^{14} molecules/ cm^3 .

3.4. Kinetics of Surface-Bound Benzo[a]pyrene on Salt Aerosols. Kinetic experiments were performed on both organic and salt aerosols to investigate the substrate effect on the kinetics of surface-bound BaP and ozone. Dry sodium chloride aerosols were used as the surrogate solid salt aerosol substrate because they are highly involatile (i.e., would not suffer from evaporation in the BaP coating region), are easily made, and have similar properties to ammonium sulfate aerosols. Kinetics were performed with dry sodium chloride particles with ozone concen-

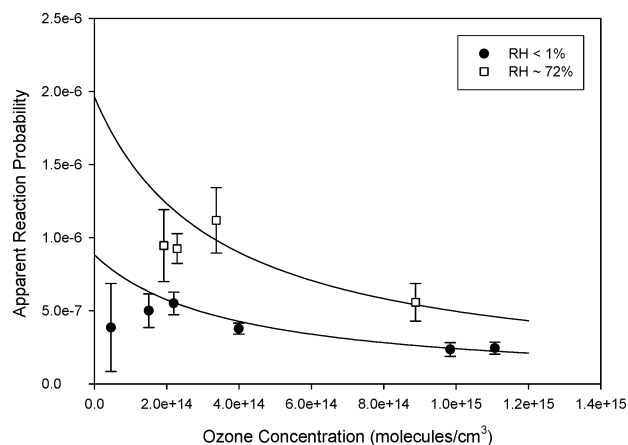


Figure 7. Ozone reaction probability as a function of gas-phase ozone concentration under dry conditions (black circles) and at 72% RH (open squares). The apparent reaction probabilities were calculated from eq 5. Equation 6 was used to obtain the curve of best fit.

trations up to 7.63×10^{14} molecules/ cm^3 . Within our experimental precision, no reaction was observed. The slowest kinetics that can be observed with our current experimental setup is $3.0 \times 10^{-3}\text{s}^{-1}$, which is the typical error of the pseudo-first-order rate constants for kinetics performed on azelaic acid aerosols under dry conditions. This value was taken as an upper limit for the pseudo-first-order rate constant for BaP loss by ozone on sodium chloride aerosols.

Although, in our study no reaction between surface-adsorbed BaP and ozone was observed on sodium chloride aerosols, an upper limit for K_{O_3} was calculated. We assumed a linear dependence of the pseudo-first-order rate coefficient on ozone concentration. Therefore, the Langmuir–Hinshelwood model described by eq 4 was modified so K_{O_3} could be obtained

$$k_{\text{obs}}^I = k_{\text{max}}^I K_{O_3}[\text{O}_3] \quad (7)$$

The k_{max}^I was taken to be the average k_{max}^I from our study and that of Poschl et al.¹⁴ (0.032s^{-1}) and the upper limit on k_{obs}^I on NaCl aerosols was used as the k_{obs}^I at the highest concentration that we investigated. Based on these assumptions an upper limit of $K_{O_3} < 1.2 \times 10^{-16}\text{cm}^3$ was obtained for sodium chloride aerosols.

4. Discussion

4.1. Reaction Kinetics and Mechanism under Dry Conditions. In this study, the kinetics between surface-adsorbed BaP and ozone was observed to be first order with respect to BaP under both dry and 72% RH conditions. There was no effect of BaP fractional surface coverage on the kinetics in the submonolayer regime. Furthermore, the plot of k_{obs}^I as a function of $[\text{O}_3]_g$ was consistent with the Langmuir–Hinshelwood reaction

mechanism as first suggested by Poschl et al.¹⁴ A reaction via this mechanism involves one species (i.e., BaP) that is strongly adsorbed to the particle surface and a second gas-phase species (i.e., ozone) that is at equilibrium with the gas phase and the particle surface. The reaction is a two-step process, with the adsorption of the gas-phase species followed by a surface reaction. As a result, the rate of the reaction is dependent on the concentration of both the surface and gas-phase species. In contrast, a linear dependence of the pseudo-first-order rate coefficient and ozone was observed in the studies by Alebic-Juretic et al.¹⁰ and Wu et al.¹¹ The ozone concentration ranges used in their studies (0.05–0.400 ppm and 0–1.5 ppm, respectively) fall within the linear regime of this current study. Therefore, behavior consistent with a Langmuir–Hinshelwood reaction mechanism may have been observed if these studies had been carried out over a larger ozone concentration range.

The K_{O_3} for azelaic acid aerosols and soot aerosols¹⁴ under dry conditions were $K_{O_3} = (1.2 \pm 0.4) \times 10^{-15}$ and $(2.8 \pm 0.2) \times 10^{-13}$ cm³, respectively (Table 2). The K_{O_3} for azelaic acid aerosols is lower than that of soot by over 2 orders of magnitude,¹⁴ which may be attributed to decreased partitioning of ozone to azelaic acid aerosols. However, the k_{\max}^I is 3 times greater on dry azelaic acid aerosols than on soot. This suggests that the rate of the elementary reaction between surface-adsorbed BaP and ozone is faster on azelaic acid aerosols and is subject, to some degree, to a substrate effect also. In terms of the overall reaction mechanism, this implies that there is decreased partitioning of ozone onto the azelaic acid aerosols compared to the soot aerosols, but once the ozone is on the particle the reaction proceeds at a slightly faster rate on azelaic acid aerosols.

To further examine the substrate effect, we estimated the K_{O_3} for other studies of surface-bound BaP on different substrates that have been used in the literature. We used the same procedure to calculate K_{O_3} as we did for the sodium chloride aerosols. In the studies by Alebic-Juretic et al.¹⁰ and Wu et al.,¹¹ a linear dependence of K_{O_3} on ozone concentration was also observed therefore, eq 7 was rearranged to yield

$$\frac{k_{\text{obs}}^I}{[O_3]} = k_{\max}^I K_{O_3} \quad (8)$$

where $k_{\text{obs}}^I/[O_3]$ is the second-order rate coefficient. Therefore, the K_{O_3} could be estimated using the second-order rate coefficient determined in their studies. Table 2 summarizes the K_{O_3} and k_{\max}^I obtained from various studies of PAHs on different substrates. On the basis of the different values of K_{O_3} in the azelaic acid and soot studies, we hypothesize that the greatest role of the substrate effect is the partitioning of ozone to a given particle surface. With the assumption that the k_{\max}^I was the same for both silica substrates, the difference in the estimated K_{O_3} for both types of silica supports this. Fused silica has been described to have an amorphous crystal structure,²¹ whereas the nonactivated silica gel was approximated by a cubic structure in the study by Alebic-Juretic et al.¹⁰ The lower K_{O_3} value for the nonactivated silica gel may be explained by greater partitioning of ozone to amorphous silica, which may be better able to trap ozone.

As previously calculated, the upper limit for K_{O_3} on sodium chloride aerosols was 1.2×10^{-16} cm³. We postulate that no reaction was observed between surface adsorbed BaP and ozone because of the small K_{O_3} . In support of this hypothesis, we note that Alebic-Juretic et al.²² investigated the destruction of ozone on solid sodium chloride particles in a fluidized bed reactor. Sodium chloride had no observed effect on ozone decomposi-

tion, which may be a result of decreased partitioning of O₃ to the sodium chloride aerosols. Taking the analogy further, we also note that carbonaceous soot substrates are those on which ozone is most easily decomposed,²³ whereas other solid surfaces where the uptake coefficients are significantly smaller include silica and solid organics. We suggest that this range in reactivity may be driven in part by the affinity that ozone has for these different surfaces, i.e., to decompose ozone must first bind to the surface and it is to soot surfaces that ozone has the highest affinity.

In general, these results highlight the importance of particle substrate selection when modeling the kinetics of surface-bound BaP and other particle-bound PAHs. Based on the experimental studies and the literature analysis presented above, the ordering of the partitioning of ozone onto different particle substrates may be described as follows: elemental carbon > fused silica > nonactivated silica gel > solid organic carbon > inorganic salts.

To conclude this section, we note that a small trend of decreasing uptake coefficients with increasing ozone concentration was observed (Figure 7). Other studies of the reaction of surface-bound PAHs and ozone on soot aerosols¹⁴ and organic films¹⁵ have also exhibited a similar, although somewhat stronger, trend between uptake coefficients and ozone concentration. The curve of best fit for Figure 7 was obtained using eq 6, which is the form of the uptake coefficient when the reaction is described by the Langmuir–Hinshelwood reaction mechanism. The physical interpretation of this observed trend of decreasing uptake coefficient with increasing ozone concentration may be explained by looking at the definition of the uptake coefficient, which is merely a ratio of the rate of the surface reaction to the total number of collisions with the surface

$$\gamma = \frac{R_r}{N_S} \quad (9)$$

where R_r is the rate for ozone loss on the surface and N_S is the collision frequency of ozone with the surface. In the limit of saturated ozone surface coverage, it is assumed that the rate of the surface reaction remains unchanged. However, at higher ozone concentrations, although the rate of the surface reaction is constant, there are more collisions between gas-phase ozone and the particle surface. Therefore, according to eq 9, the uptake coefficient would decrease correspondingly, with increasing ozone concentration.

The ozonation of surface-bound PAHs are not the only systems to exhibit this inverse dependence of uptake coefficient on gas-phase reactant concentration. Sullivan et al.²⁴ observed a similar trend in their study of the decomposition of ozone on thin alumina films, as did Hanisch and Crowley²⁵ in their study of ozone decomposition on Saharan dust. This suggests that the initial step in both processes, i.e., decomposition of ozone on solid metal oxide surfaces and reaction of ozone with adsorbed PAHs, may proceed via the same initial step of ozone adsorbing to the surface via a Langmuir type mechanism.

4.2. Reaction Kinetics and Mechanism at High Relative Humidity. The kinetics of surface-bound BaP on organic aerosols at 72% RH were also investigated. An enhancement compared to dry conditions was observed, although the basic Langmuir–Hinshelwood form of the kinetic results was preserved (Figure 6). In this study, values of $K_{O_3} = (1.2 \pm 0.4) \times 10^{-15}$ and $(2.8 \pm 1.4) \times 10^{-15}$ cm³ were obtained under <1% RH and 72% RH conditions, respectively. Furthermore, $k_{\max}^I(<1\% \text{ RH}) = (0.048 \pm 0.008) \text{ s}^{-1}$ and $k_{\max}^I(72\% \text{ RH}) =$

(0.060 ± 0.018) s⁻¹. The higher K_{O_3} and k_{\max}^1 at 72% RH results in shorter lifetimes with respect to ozone for surface-bound BaP. For example, with an ozone concentration of 100 ppb the lifetime of surface-bound BaP is 84 min under dry conditions. This reduces to 28 min at 72% RH.

The enhancement in the kinetics at high RH is primarily driven by the increased affinity of ozone for the wet azelaic acid surface rather than by an increase in the surface rate constant between adsorbed ozone and surface-bound BaP; that is, with increasing RH, K_{O_3} increases by 230%, whereas k_{\max}^1 increases by only 25%. This behavior is consistent with the literature where it has been concluded that water does not appear to be involved in the ozonation of BaP as it is in the ozonation of other PAHs.^{26,27} In general, a mechanism for the oxidation of BaP by ozone in the condensed phase has been proposed by Moriconi et al.²⁸ The first step of the reaction involves an electrophilic attack of ozone to the carbon positions with the lowest electron density. Most reactions of ozone with olefins then form an initial cyclic primary ozonide; however, this is an unlikely process for the ozonation of BaP because the required positions are too far apart for ozone to form a bridge across.

Therefore, assuming a similar reaction mechanism for the ozonation of surface-bound BaP as there is in the condensed phase, we proceed under a model where water is not directly involved in the surface-phase reaction. By inference it must instead be enhancing the overall kinetics by providing a surface to which ozone has a higher affinity. The current understanding in the community is that water adsorbs to oxidized organics in roughly monolayer quantities at RHs similar to those used in our enhanced RH experiments.^{29,30} Although the water is most probably not present as a uniform layer on the surface, more likely instead in the form of islands or at corrugations,²⁹ we nevertheless believe that the ozone has a higher affinity for these forms of surface water than for the bare azelaic acid surface itself.

Upon examination of Table 2, there are two extremes represented for the ozone gas-to-surface equilibrium constant (K_{O_3}). The soot particles represent a hydrophobic, nonpolar surface, whereas the sodium chloride particles represent a polar, ionic one. It is possible that the wet azelaic acid particles can be thought of as having a less polar surface, due to the presence of water, than that of the dry azelaic acid particles. Therefore, assuming ozone prefers nonpolar surfaces, ozone will have a higher affinity for the wet azelaic acid surface compared to the dry. This will translate to enhanced kinetics, since, as we suggest, the rate of the reaction is primarily driven by the partitioning of the ozone onto the particle's surface. Furthermore, Mmerekki et al.¹⁵ also observe similar behavior for the reaction of anthracene and ozone on different film surfaces. They report an increase in the rate on the octanol-coated aqueous surface compared to the pure water surface. Given that octanol is less polar than water, these observations are consistent with our own, if we assume that all PAHs behave similarly.

A similar conclusion has been reached by Poschl,⁶ who noted a kinetic enhancement effect in experiments at RHs higher than 50%, when examining the reactivity of ozone with BaP adsorbed on soot. Conversely, at lower RHs of 25%, Poschl et al.¹⁴ observed a suppression in the same reaction due to competitive adsorption between ozone and water. Motivated by Poschl et al.'s¹⁴ work, we also performed some preliminary experiments at 25% RH on azelaic acid aerosols with an ozone concentration of 9.52×10^{14} molecules/cm³. Our results revealed a similar enhancement in kinetics at 25% RH compared to 72% RH. We attribute this difference in behavior to the hygroscopic nature

of azelaic acid, which may already be sufficiently modified at 25% RH for enhancement to be observed. Conversely, graphitic soot is a hydrophobic surface and so it is quite possible that there is not sufficient water on a soot surface at 25% RH to enhance ozone uptake. Instead, as described by Poschl et al.,¹⁴ competitive adsorption for common surface sites between low levels of water and the ozone appears to explain these results.

There have been other conflicting observations regarding the effect of increased relative humidity on the degradation of PAHs by ozone. On one hand, Kamens et al.¹³ investigated PAH loss on atmospheric soot aerosols in the presence of natural sunlight in outdoor chambers. They reported faster BaP decays at higher relative humidities, which is in agreement with our observations. Other degradation pathways that include direct PAH photolysis, molecular oxidation, and hydroxyl attack were used to explain their observations, although we suggest that effect could be due to the mechanism described above. In our study, the elevated humidity experiments were performed in the dark where these photochemical pathways would be minimized. Conversely, we point out that there are also studies where decreased PAH reactivity was observed at higher relative humidities. In particular, Pitts and co-workers³¹ observed this effect while studying the reactions of PAHs on filters or ambient particulate organic matter.

5. Atmospheric Implications and Conclusions

We have shown in this work that the reaction between ozone and surface-adsorbed BaP appears to follow a Langmuir–Hinshelwood reaction mechanism following on from the work of Poschl et al.,¹⁴ who were the first to demonstrate this. It is quite possible that previous studies of the reaction on other substrates such as silica gel and glass fiber filters also would have displayed Langmuir–Hinshelwood kinetics had the studies been performed over a wider range of ozone concentrations. In addition, we postulate that the primary factor which determines the lifetime of surface-bound BaP from aerosol to aerosol type, at least for our case of solid particles, is the ability of the ozone to bind to the substrate. As an example, in the present study, the lifetime of BaP on azelaic acid particles at 100 ppb of ozone is approximately 84 min, whereas it is >13 days on solid sodium chloride aerosols under dry conditions. These lifetimes indicate that the BaP and any other low volatility products may be subject to further oxidation by atmospheric oxidants such as OH, NO_x, and SO_x. By examining our own kinetics and others in the literature, we conclude that the ordering of the partitioning of ozone onto different particle substrates may be described as follows: elemental carbon > fused silica > nonactivated silica gel > solid organic carbon > inorganic salts. The difference in affinity of ozone for different substrates may also explain why ozone reactivity with bare soot surfaces is significantly higher than with other solids, such as the metal oxides. In particular, the initial step in the decomposition of ozone on these surfaces probably involves a reversible adsorption step, just as required in the reactions between ozone and adsorbed PAHs.

The experiments conducted at elevated relative humidity resulted in an enhancement in the observed kinetics. We believe that this enhancement again reflects a substrate effect rather than a change in the rate of reaction between adsorbed ozone and BaP. In particular, ozone binds more strongly to a solid organic surface which contains monolayer quantities of adsorbed water than it does to a dry surface. These results illustrate that relative humidity must be taken into consideration when assessing the lifetimes of these molecules in the atmosphere.

Acknowledgment. We thank Dan Mathers of the Analest facility for use of the HPLC with fluorescence detector. We also thank NSERC, TSRI, and ASC-PRF for funding this project.

References and Notes

- (1) Finlayson-Pitts, B. J.; Pitts, J. N., Jr. *Chemistry of the Upper and Lower Atmosphere: Theory Experiments and Applications*; Academic Press: Toronto, 2000.
- (2) Schwartz, J.; Laden, F.; Zanobetti, A. *Environ. Health Persp.* **2002**, *110*, 1025–1029.
- (3) Pitts, J. N., Jr; van Cauwenberghe, K. A.; Grosjean, D.; Schmidt, J. P.; Fritz, D. R.; Belser, W. L., Jr; Knudson, G. B.; Hynds, P. M. *Science* **1978**, *202*, 515–519.
- (4) Pitts, J. N., Jr; Lokensgard, D. M.; Ripley, P. S.; Cauwenberghe, K. A.; Van Vaecck, L.; Shaffer, S. D.; Thill, A. J.; Belser, W. L. *Science* **1980**, *210*, 1347–1349.
- (5) Kotzick, R.; Panne, U.; Niessner, R. *J. Aerosol Sci.* **1997**, *28*, 725–735.
- (6) Poschl, U. *J. Aerosol Med.* **2002**, *15*, 203–212.
- (7) Lane, D. A.; Katz, M. *Adv. Environ. Sci. Technol.* **1977**, *8*, 137–154.
- (8) Grosjean, D.; Fung, K.; Harrison, J. *Environ. Sci. Technol.* **1983**, *17*, 673–679.
- (9) Korfmacher, W. A.; Wehry, E. L.; Mamantov, G.; Natusch, D. F. *S. Environ. Sci. Technol.* **1980**, *14*, 1094–1099.
- (10) Alebic-Juretic, A.; Cvitas, T.; Klasinc, L. *Environ. Sci. Technol.* **1990**, *24*, 62–66.
- (11) Wu, C.-H.; Salmeen, I.; Niki, H. *Environ. Sci. Technol.* **1984**, *18*, 603–607.
- (12) Rajagopalan, R.; Vohra, K. G.; Mohan Rao, A. M. *Sci. Total Environ.* **1983**, *27*, 33–42.
- (13) Kamens, R. M.; Guo, Z.; Fulcher, J. N.; Bell, D. A. *Environ. Sci. Technol.* **1988**, *22*, 103–108.
- (14) Poschl, U.; Letzel, T.; Schauer, C.; Niessner, R. *J. Phys. Chem. A* **2001**, *105*, 4029–4041.
- (15) Mmereki, B. T.; Donaldson, D. J. *J. Phys. Chem. A* **2003**, *107*, 11038–11042.
- (16) *Yaw's Handbook of Thermodynamic and Physical Properties of Chemical Compounds*; Knovel: New York, 2003.
- (17) . *Spectral Atlas of Polycyclic Aromatic Compounds*; Kluwer Academic Publishers: Boston, 1988.
- (18) Murray, J. J.; Pottie, R. F.; Pupp, C. *Can. J. Chem.* **1974**, *52*, 557–563.
- (19) Atkins, P. W. *Physical Chemistry*, 5th ed.; W. H. Freeman and Company: New York, 1994.
- (20) Ammann, M.; Poschl, U.; Rudich, Y. *Phys. Chem. Chem. Phys.* **2003**, *5*, 351–356.
- (21) *Electro-Optics Handbook*, 2nd ed.; McGraw-Hill: New York, 2000.
- (22) Alebic-Juretic, A.; Cvitas, T.; Klasinc, L. *Environ. Monit. Assess.* **1997**, *44*, 241–247.
- (23) Longfellow, C. A.; Ravishankara, A. R.; Hanson, D. R. *J. Geophys. Res.* **2000**, *105*, 24345–24350.
- (24) Sullivan, R. C.; Thornberry, T.; Abbatt, J. P. D. *Atmos. Chem. Phys. Discuss.* **2004**, *4*, 1977–2002.
- (25) Hanisch, F.; Crowley, J. N. *Atmos. Chem. Phys.* **2003**, *3*, 119–130.
- (26) Bailey, P. S. In *Ozonation in Organic Chemistry*; Academic Press: Toronto, 1982.
- (27) Mmereki, B. T.; Donaldson, D. J.; Gilman, J. B.; Eliason, T. L.; Vaida, V. *Atmos. Environ.* **2004**, *38*, 6091–6103.
- (28) Moriconi, E. J.; Rakoczy, B.; O'Connor, W. F. *J. Am. Chem. Soc.* **1961**, *83*, 4618–4623.
- (29) Thomas, E.; Rudich, Y.; Trakhtenberg, S.; Ussyshkin, R. *J. Geophys. Res.* **1999**, *104*, 16053–16059.
- (30) Demou, E.; Visram, H.; Donaldson, D. J.; Makar, P. A. *Atmos. Environ.* **2003**, *37*, 3529–2537.
- (31) Pitts, J. N., Jr.; Paur, H.-R.; Zielinska, B.; Arey, J.; Winer, A. M.; Ramdahl, T.; Mejia, V. *Chemosphere* **1986**, *15*, 675–685.